An Analytical Approach to Oxide Scale Adhesion on Si-Containing Recycled Steel for Process Waste Reduction

Seksan Singthanu
Program in Industrial Management Engineering, Faculty of Industrial Technology, Rajabhat Rajanagarindra University, Thailand
ssc.sek9@gmail.com

Thanasak Nilsonthi
High Temperature Corrosion Research Centre and Department of Materials and Production Technology Engineering, Faculty of Engineering, King Mongkut's University of Technology North Bangkok, Thailand
thanasak.n@eng.kmutnb.ac.th (corresponding author)

Received: 19 November 2025 | Revised: 24 December 2025 | Accepted: 29 December 2025

 DOI: https://doi.org/10.48084/etasr.16384

ABSTRACT

This study investigates the oxide scale adhesion behavior on Si-containing recycled hot-rolled steel to provide insights for process waste reduction during descaling. Steel samples with varying silicon (Si) content (0.01 to 0.3 wt.%) were re-oxidized in a 17% H_2O-N_2 atmosphere at 700-900 °C for 1 min. Quantitative and qualitative assessment techniques were integrated. Phase analysis confirmed hematite (Fe_2O_3) and magnetite (Fe_3O_4) formation. Microstructural analysis revealed that scale thickness decreased with rising Si content but increased with temperature. Adhesion was evaluated using an innovative macro-tensile test combined with real-time observation (CCD camera). Quantitative fracture mechanics, utilizing the strain initiating the first scale spallation, were used to calculate the mechanical adhesion energy. The results showed that higher Si content significantly enhanced scale adhesion, with mechanical adhesion energy values being in the 20-40 J/m^2 range. This strong adherence is attributed to the potential formation of an Si-rich oxide phase at the steel/scale interface. This integrated assessment confirms that while high Si content promotes a thinner scale (reducing material waste), it simultaneously increases scale tenacity, significantly increasing descaling energy (process waste). For producers, the results emphasize the necessity of tightly controlling Si content in recycled steel inputs below a critical threshold (e.g., 0.2 wt.%) to optimize downstream operations and minimize energy waste.

Keywords-recycled steel; oxide scale adhesion; silicon; analytical approach; process waste reduction

I. INTRODUCTION

The global steel industry, relying on recycled steel feedstock to meet sustainability and resource efficiency goals, faces challenges in process control and product quality. A phenomenon governing hot-rolled steel processing is the formation and adhesion of the oxide scale on the strip surface. This scale layer is critical; its characteristics directly impact final surface quality and the cost-intensive descaling process [1, 2]. While poor scale adhesion can lead to undesirable spallation and defects, excessive adhesion significantly compromises descaling efficiency, demanding high mechanical energy input typically via high-pressure water jets, thereby increasing process waste in the form of elevated energy consumption and operational costs [3, 4].

The effective management of oxide scale adhesion is complicated by the presence of tramp elements, particularly silicon (Si), which is commonly introduced through recycled inputs. Si is well-established as an element that segregates to the steel-scale interface, altering the local oxidation kinetics by forming thin, protective layers of SiO_2 or Fe_2SiO_4 [5, 6]. This segregation often results in a thinner overall scale (benefiting material conservation) but simultaneously promotes a highly tenacious bond [7, 8]. Optimizing industrial operations requires quantifying the trade-off between material loss and energy consumption, as traditional qualitative metrics often lack precision. Control over product performance is dictated by the steel's inherent microstructure and alloying effects. For instance, Rare Earth (RE) additions to Cu-bearing weathering steel significantly improve corrosion resistance by replacing elongated manganese sulfide inclusions with spherical RE-oxysulfides, thereby reducing pitting susceptibility. These

elements also promote a compact, protective rust layer dominated by stable goethite [9]. Thermodynamically, RE elements exhibit a high affinity for oxygen and sulfur, effectively reducing impurities and modifying inclusions during solidification. Achieving high RE recovery requires specific addition methods, such as plunging or encapsulation, combined with stable magnesia refractories [10]. Furthermore, specific heat treatments, like intercritical annealing of 5Mn steel, can develop a sub-micron laminated structure of tempered martensite and reversed austenite. Mn enrichment stabilizes the austenite and triggers the Transformation-Induced Plasticity (TRIP) effect, markedly enhancing low-temperature toughness [11].

Complementary to microstructural effects, the mechanical stability of the scale/steel interface is significantly influenced by geometry and residual stresses. Finite element simulations indicate that tensile and shear stresses, amplified by interface roughness and thermal mismatch during cooling, are the primary drivers of scale spallation [12]. Furthermore, the continuous growth in research regarding the fracture, fatigue, and structural integrity of metallic materials underscores the ongoing importance of disseminating significant advances in these fields to better understand and predict material performance under complex loading conditions [13]. Consequently, when investigating scale adhesion under tensile loading, it is crucial to understand how the scale fracture behavior is coupled with the substrate plastic deformation behavior, especially since the scale must sustain the imposed strain from the ductile substrate.

To bridge this gap, this research employs an analytical approach combining methods from both material science and quantitative fracture mechanics. The objectives of this study are: to conduct a microstructural analysis to correlate Si concentration and processing temperature (700-900 °C) with the scale phase composition and thickness; to quantitatively assess the mechanical adhesion energy using an innovative macro-tensile test coupled with real-time visual observation and quantitative fracture mechanics; and to establish an evidence-based recommendation for hot-rolled steel producers regarding the optimal Si content control, necessary for process waste reduction through energy optimization during the descaling phase. The integrated findings presented in this study provide highly reliable data on the interfacial bonding strength, unique to recycled steel systems, offering a technical foundation for balancing material efficiency with energy sustainability.

II. MATERIALS AND METHODS

A. Steel Sample Preparation

The investigation utilized hot-rolled steel strips with a uniform thickness of 3.2 mm obtained from a recycling-based production route. The process of hot rolling resulted in steel strips with finishing temperatures of 860 °C and coiling temperatures of 650 °C. To evaluate the effect of tramp element content, four distinct Si concentrations were selected: 0.01, 0.10, 0.20, and 0.30 wt. %. The other alloying elements generally had similar contents, with their detailed chemical composition presented in Table I.

TABLE I. COMPOSITION OF HOT-ROLLED STEEL SAMPLES (WT.%)

Steel samples	C	Si	Cu	Mn	P	S	Fe
0.01	0.17	0.01	0.01	1.05	0.02	0.01	Bal.
0.10	0.16	0.13	0.01	0.90	0.02	0.01	Bal.
0.20	0.12	0.19	0.03	1.40	0.02	0.02	Bal.
0.30	0.16	0.29	0.02	1.16	0.02	0.01	Bal.

B. Controlled Oxidation Process

Specimens were laser cut from the hot-rolled steel strips according to the ASTM E8M standard for subsequent tensile testing. The surface preparation involved polishing with SiC paper up to 1200 grade for descaling, followed by cleaning under ethyl alcohol, using an ultrasonic cleaning machine, air drying, and then immediate placement in a horizontal furnace. The oxidation process was carried out to simulate the high-temperature environment, typical of the hot-rolling finishing stages. The specimen was initially oxidized in the furnace for 1 min at temperatures of 700, 800, and 900 °C. This specific duration was chosen to establish a uniform and stable initial scale layer, providing a consistent baseline for adhesion testing. Furthermore, it allowed for the observation of early-stage Si enrichment and interface formation (such as fayalite) before the scale became excessively thick. This was conducted under a precisely controlled humid atmosphere consisting of 17% H_2O balanced with N_2 at a flow rate of 6 L/min. Following the entire oxidation period, the samples were cooled in a controlled N_2 atmosphere to room temperature. This entire process yielded uniform oxide scales for subsequent analysis. Before and after oxidizing, the samples were weighed on an electronic microbalance to determine the oxidation kinetics.

C. Microstructural and Phase Analysis

The characteristics of the formed oxide scales were analyzed using standard material characterization techniques. X-Ray Diffraction (XRD) (D8 Advance model) was employed for phase identification of the crystallographic structures present in the oxide scale. The XRD measurement conditions utilized an X-Ray generator of 40 kV and 30 mA, employing the Cu Kα line (0.15406 nm) with a scan speed of 2.00º/min and a step width of 0.02º. Microstructural characterization, including the cross-section morphologies, thickness of the oxide scale layers, and the composition of the steel/scale interface, was examined using a Scanning Electron Microscope (SEM, Quanta 450) equipped with Energy-Dispersive X-ray Spectroscopy (EDS). EDS was utilized to perform point analyses with an electron probe focused on a 1 µm spot. Furthermore, the scale thickness can be estimated based on the assumption of a pure iron substrate:

$$\text{Scale thickness } (\mu m) = \frac{\Delta m}{A} \cdot \frac{1}{M_O} \cdot M_{FeO} \cdot \frac{1}{\rho_{FeO}} \cdot 10^4 \quad (1)$$

where Δm is the mass gain (g), A is the area (cm^2), M_O is the molecular weight of oxygen (16 g/mol), M_{FeO} is the molecular weight of iron oxide (72 g/mol), and ρ_{FeO} is the density of iron oxide (5.745 g/cm^3).

D. Adhesion Measurement and Analytical Fracture Mechanics

Scale adhesion was analytically assessed using a novel, integrated macro-tensile testing approach based on the Evans criterion and the Galerie-Dupeux model [14, 15]. For the test setup, specimens were subjected to a controlled tensile load using a universal testing machine (Instron, model 5566). The geometry of the specimen used for tensile loading is illustrated in Figure 1. The tensile load applied was 10 kN with a strain rate of 0.04/s. The entire tensile test process was monitored simultaneously by a CCD camera system for real-time observation, allowing qualitative observation of the failure and identification of the exact critical strain value at which the first scale spallation event occurred. This critical strain then served as the essential input for the adhesion energy calculation. The analytical fracture mechanics approach models the scale/substrate system as an elastic layer on a plastic substrate, utilizing the measured critical strain to determine the critical strain energy release rate, which is numerically equivalent to the mechanical adhesion energy.

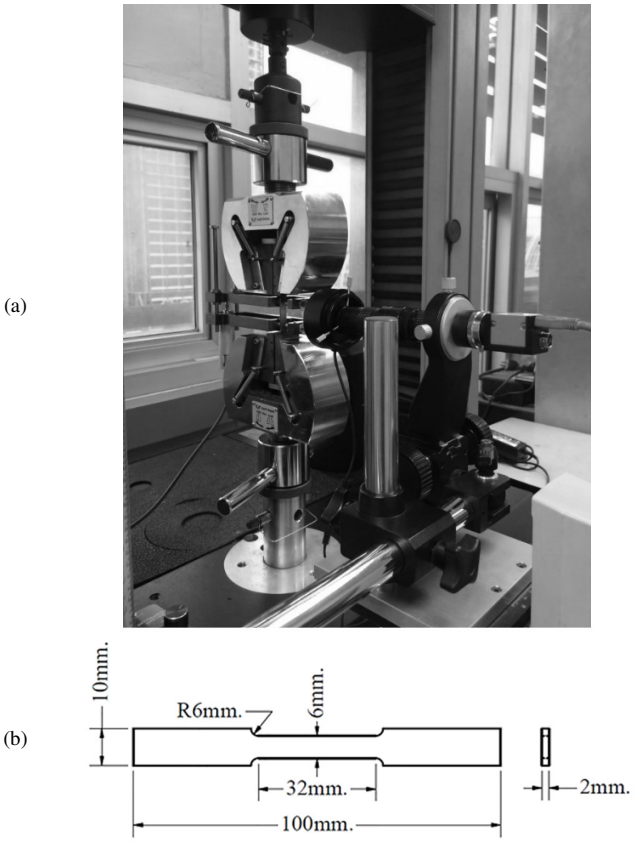

Fig. 1. Testing setup: (a) macro-tensile adhesion testing setup; (b) specimen dimensions.

This methodology allows for the quantification of the interfacial bond strength by relating the macro-scale mechanical loading to the micro-scale energy required for interface crack propagation and subsequent scale failure. To establish a quantitative metric for interfacial bonding strength, the mechanical adhesion energy was derived. This value is calculated by considering the stored strain energy (energy per unit volume) within the scale at the point of failure, normalized by the scale thickness, according to:

$$G = W_{total} \cdot t \quad (2)$$

where G is the mechanical adhesion energy (J/m^2), W_{total} is the stored energy corresponding to the area under the stress-strain curve (J/m^3), and t is the oxide scale thickness (m). The area under the stress-strain curve was utilized to calculate the stored energy of the oxide scale in both the x and y directions, as detailed by the governing equation $\int \sigma \cdot d\varepsilon$. During tensile loading, the steel substrate underwent plastic deformation while the oxide scale remained elastic until the first scale spallation event occurred. The key mechanical properties used in the calculation were Young's modulus of both steel and oxide (210 GPa), Poisson's ratio of both steel and oxide (0.3), a compressive residual stress of the oxide (-0.2 GPa), and the strain at the limit of elasticity of the oxide (0.0015). This difference in mechanical response, due to the plastic yielding of the substrate versus the elastic brittleness of the scale, creates the critical strain gradient and resultant stress concentration at the steel/scale interface, which ultimately governs the location and initiation of the first spallation event. The established mechanical constants and initial compressive residual stress are essential inputs used to model this interfacial stress state just before fracture.

III. RESULT AND DISCUSSION

The structural characteristics of the formed oxide scales were thoroughly investigated using SEM to understand the influence of the Si content. The cross-sectional SEM micrographs, displayed in Figure 2, illustrate the scale morphology for varying Si concentrations (0.01-0.3 wt.%), all oxidized at 900 °C. The examination of these specimens revealed distinct differences in the scale thickness and overall microstructure based on Si alloying content. A significant finding emerged at the 0.3 wt.% Si/scale interface, namely EDS analysis confirmed the occurrence of internal oxidation. The presence of Fe_2SiO_4 (fayalite), a Si-rich compound, marked this process, exhibiting a measurable penetration depth into the steel substrate. This formation created an intricate and tight bond at the metal-oxide boundary, which significantly influences the scale of subsequent mechanical performance.

The influence of both the Si content and the oxidation temperature on the resulting oxide layer thickness was systematically quantified, with the results presented graphically in Figure 3. The measured scale thickness, derived from SEM imaging of cross-sections, was validated through comparison against theoretical estimations, calculated using (1). Two significant trends were established: scale thickness demonstrated a direct relationship with oxidation temperature (700-900 °C) due to accelerated diffusion kinetics, while conversely exhibiting a clear inverse correlation with Si concentration, which promoted the formation of a dense, protective diffusion barrier at the metal-scale interface. Quantitatively, the steel containing only 0.01 wt.% Si exhibited the highest scale thickness, measured significantly within the

range of 2.65 to 4.15 um under the higher temperature range. In contrast, the 0.3 wt.% Si-enriched steel, representing the highest concentration studied, produced a substantially thinner scale, ranging from 0.87 to 1.60 um, confirming the potent barrier effect of elevated Si levels.

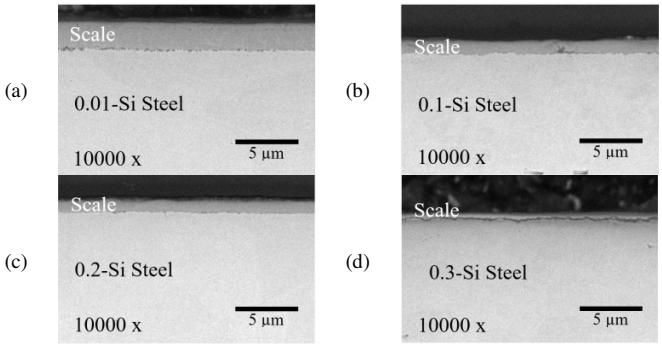

Fig. 2. Cross-sectional SEM micrographs of oxide scales formed on hot-rolled steel with varying Si content: (a) 0.01 wt.%, (b) 0.1 wt.%, (c) 0.2 wt.%, and (d) 0.3 wt.%, all oxidized at 900 °C.

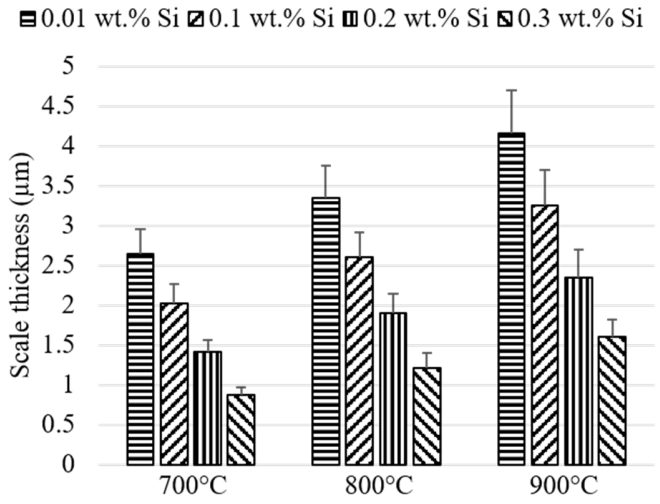

Fig. 3. Measured and calculated scale thickness as a function of Si content at different oxidation temperatures.

XRD analysis was performed on the oxide scales formed across all Si concentrations (0.01-0.3 wt.%) at the maximum tested temperature of 900 °C. The diffraction patterns, detailed in Figure 4, confirmed a consistent primary phase composition across all samples. The scale structure was composed of the outer oxides hematite (Fe_2O_3) and the inner layer magnetite (Fe_3O_4). A notable observation was the presence of significant diffraction peaks corresponding to metallic iron (Fe), which were detected beneath the oxide layers. Considering the Fe-O phase diagram, the appearance of these Fe peaks can be directly correlated with the decomposition of the wustite (FeO) phase into magnetite and Fe metal. This decomposition is thermodynamically favored at temperatures below approximately 570 °C, a condition likely met during the controlled cooling phase of the specimens. The hematite layer typically occupies the outermost surface directly exposed to the oxidizing atmosphere, followed by the magnetite layer, which adheres directly to the steel substrate. An evaluation of the peak intensities showed an important trend: the intensity of the detected Fe peaks increased proportionally with higher Si content in the steel substrate. This suggests that the presence of elevated Si levels influences the stability or the final structure of the intermediate FeO layer during cooling, potentially leading to a more pronounced decomposition and metallic Fe precipitation beneath the scale.

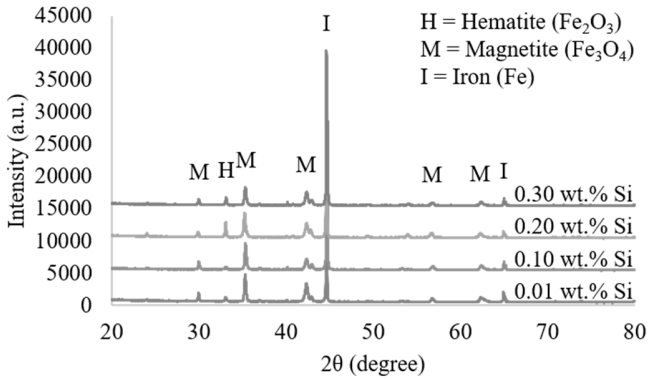

Fig. 4. Comparative XRD patterns of oxide scales formed on Si-containing hot-rolled steel oxidized at 900 °C.

The mechanical adhesion of the oxide scale was characterized quantitatively by monitoring the critical strain at which the initial scale spallation event was observed. This parameter is significant for quantitatively comparing the interfacial bond strength of the scale across varying Si contents and simulated finishing stage temperatures. During tensile loading, the ductile steel substrate undergoes significant plastic deformation, while the brittle oxide scale, unable to accommodate this large imposed strain difference, fails. This strain mismatch between the substrate and the scale is the fundamental driving force causing the scale to detach and spall away from the metal. The internal stresses already present in the scale, primarily generated by the Coefficient of Thermal Expansion (CTE) mismatch upon cooling from the oxidation temperature, are further amplified by the external tensile load, driving the scale toward failure. The time-dependence of this initial fracture initiation provides insights into the scale tenacity; the velocity at which this initial spallation propagated was inversely proportional to the scale adhesion strength, meaning that lower intrinsic adhesion resulted in a more rapid and catastrophic fracture initiation. The entire process, with a precise focus on the center of the specimen where stress concentration is maximized, was captured using a high-resolution CCD camera for real-time observation and accurate critical strain determination, providing the necessary data input for calculating the mechanical adhesion energy using fracture mechanics models.

Figure 5 illustrates the behavior of the oxide layer on the 0.3 wt.% Si steel subjected to increasing tension. Initially, fine transverse cracks oriented perpendicular to the applied tensile axis were observed, which subsequently propagated and led to the major first-scale spallation. Visual analysis confirmed that

the total area of scale spallation intensified as the global strain increased. This phenomenon was easily identified in the CCD footage, as the regions where the oxide layer had detached and fallen away appeared as distinct dark (black) areas on the steel substrate.

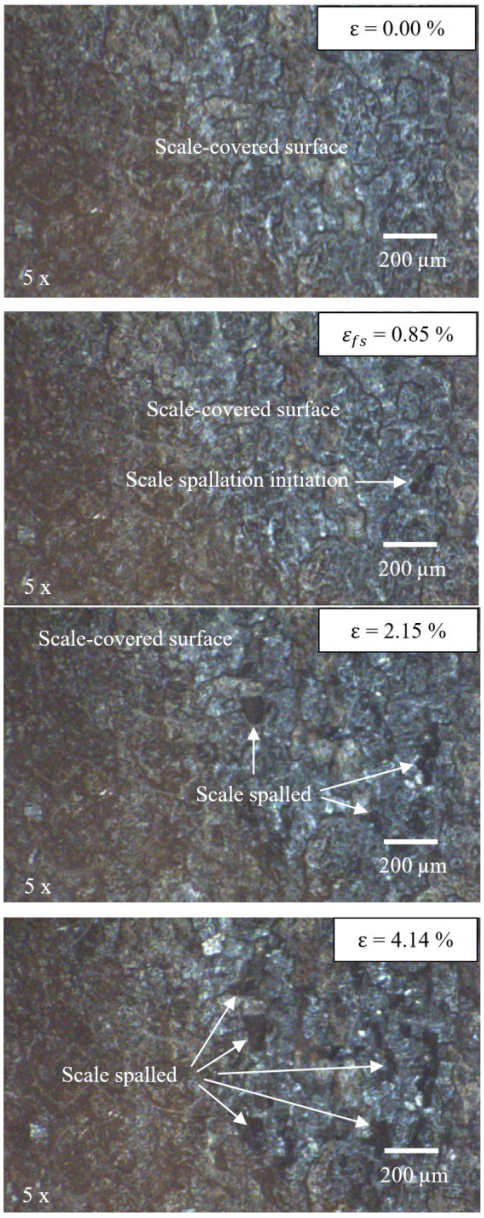

Fig. 5. Failure morphology of the oxide layer on 0.3 wt.% Si steel under imposed strain, following oxidation at 900 °C.

The critical strain required to initiate the first scale spallation for all Si-containing hot-rolled steel specimens at varying oxidation temperatures is presented in Figure 6. This measured parameter, which defines the point of interfacial failure, revealed two crucial trends. A consistent inverse relationship was established between the oxidation temperature and the critical strain value. Higher processing temperatures decreased the strain tolerance of the oxide scale before initial failure. This reduction in critical strain suggests that elevated temperatures either increase the inherent internal stress within the scale or weaken the metal-oxide bond, making the scale more susceptible to cracking under minimal deformation. From a mechanical perspective, this occurs because the total stress in the oxide scale is a combination of the internal thermal stress (created during cooling) and the external tensile strain. The thermal stress acts like an initial pre-load on the scale. At higher temperatures, this internal pre-load is stronger. That is, it takes very little additional pulling force to reach the breaking point and start the spallation. Once the peeling begins, the speed at which it spreads depends on how much of this combined energy has been stored. However, the Si in the steel forms a fayalite layer that acts like a mechanical anchor at the interface. This anchoring effect strengthens the bond, which not only delays the start of the spallation but also slows down the speed at which the scale peels away from the steel surface.

In contrast, increasing the Si alloying content substantially enhanced the critical strain for spallation. This observation confirms that Si significantly improves the mechanical tenacity of the scale-substrate interface. Specifically, the 0.3 wt.% Si steel exhibited the highest critical strain values across all temperatures, indicating a superior adhesive bond compared to lower Si counterparts. This critical strain, combined with the measured oxide scale thickness, served as the main input for calculating the mechanical adhesion energy. This calculated energy value provides the quantitative metric for interfacial adhesive strength, directly representing the bonding tenacity between the formed oxide layer and the steel substrate.

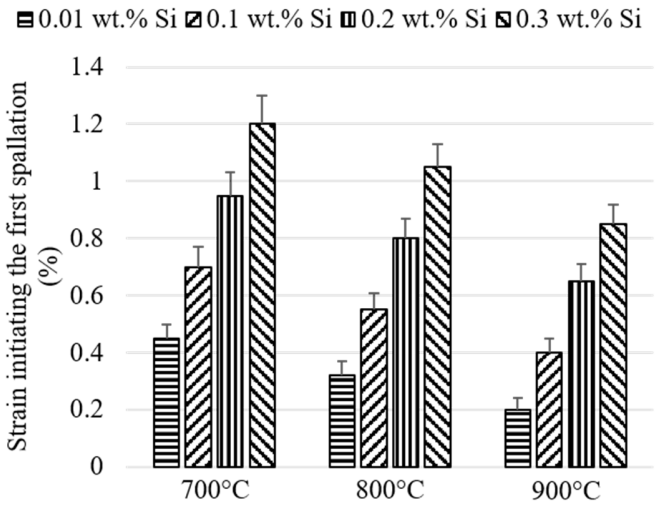

Fig. 6. Strain initiating the first spallation of the Si-containing hot-rolled steel oxidized at 700, 800, and 900 °C.

The calculated mechanical adhesion energy, a direct quantitative measure of interfacial bond strength, is illustrated as a function of the Si content and oxidation temperature in Figure 7. The results confirmed that scale adhesion is a significant function of both processing temperature and Si concentration. A positive correlation was established; the adhesion energy increased significantly with increasing Si

content. The presence of elevated Si promotes the formation of a protective oxide layer (likely fayalite, Fe_2SiO_4) at the innermost scale-steel interface. This Si-rich layer acts as a chemical and physical glue, effectively blocking rapid ion diffusion and substantially enhancing the bond strength of higher Si-containing steel, thereby increasing its resistance to mechanical detachment. Conversely, the data showed that increased oxidation temperature led to an important decrease in scale adhesion.

This effect was pronounced in scales formed at higher temperatures under saturated water vapor. This reduction is primarily linked to the diffusion of interstitial oxygen through the scale, which promotes continued internal oxidation or alters the phase stability at the interface. The overall adhesive strength is compromised by the accumulation of residual stress. The growth and subsequent cooling of the oxide layer generate significant compressive stress between the innermost oxide layer and the steel substrate. This built-up residual stress predisposes the scale-substrate system to cracking and spallation when subjected to external forces (such as those applied during the tensile test or the hot-rolling process). Consequently, scales formed under conditions that heighten internal stress (high temperature, high humidity) are more easily detached.

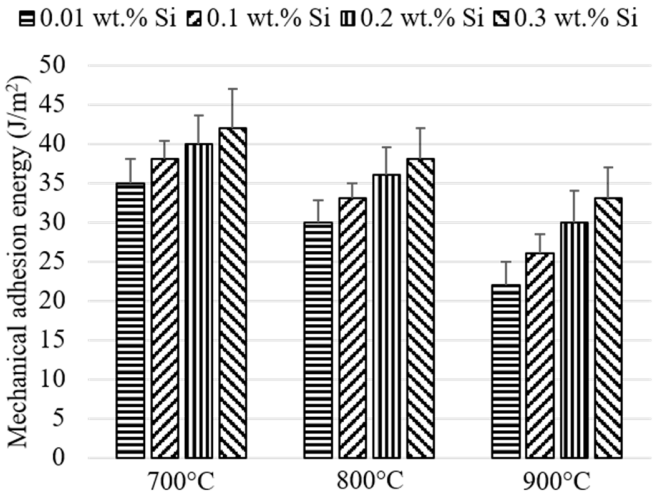

Fig. 7. Mechanical adhesion energy of the Si-containing hot-rolled steel oxidized at 700, 800, and 900 °C.

(a)

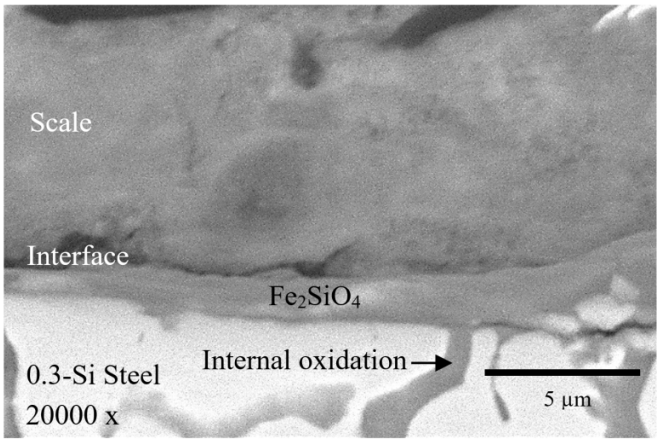

(b)

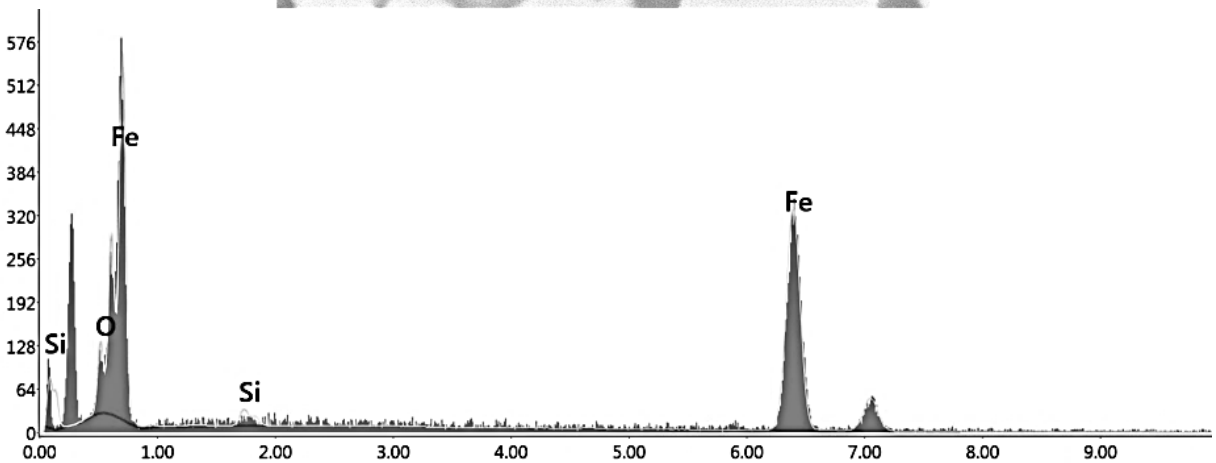

Fig. 8. Interfacial and morphological study of high-Si steel oxidized at 900 °C: (a) SEM cross-section reveals scale structure, (b) corresponding EDS patterns detail element distribution at the 0.3 wt.% Si/steel boundary.

According to the results, when the Si content increases in the hot-rolled steel, it tends to increase the scale adhesion. Figure 8 shows that the SEM-EDS revealed that the interfacial layer of steel with 0.3 wt.% Si has an oxide containing Si, possibly as SiO_2 or Fe_2SiO_4, because the EDS spectrum includes the peaks of Fe, O, and Si. A Si-enriched oxide present at the steel-scale interface caused an increase in steel passivity and adhesion during the production of the Si-oxide phase. The Si-oxide-formed internal subscale was a barricade to the production of external oxide. Moreover, the Si-oxide layer at the steel-scale interface was also shown to increase scale adhesion. When the Si content in steel increased, it resulted in internal oxidation, which was not seen in lower Si-containing steel. This is because a diffusion that was controlled by dissolved oxygen became insufficient during the oxidation of the Si element in the steel, which was unavoidable in the case of Si-containing steel oxidized at high temperatures in a water vapor atmosphere. This internal oxidation layer significantly modifies the mechanical behavior of the scale-substrate interface. From a mechanical perspective, the Si-enriched interface acts as a buffer zone that redistributes local strain mismatch.

The irregular, root-like structures of the internal oxide provide a mechanical anchoring effect, which increases the critical interfacial fracture toughness. This modification alters the fracture behavior under tensile loading; while internal thermal stresses act as a pre-load that promotes spallation, the anchoring effect of the fayalite-rich layer effectively counters this by requiring higher external energy to propagate cracks along the interface. Consequently, the 0.3 wt.% Si steel can accommodate significantly higher strain before failure compared to lower Si-containing steels. The oxide containing Si existing at the steel-scale interface promoted the mechanical adhesion of scale to the steel substrate, thereby worsening the picklability of scale during the descaling process in the hot rolling line.

IV. CONCLUSION

This investigation efficiently quantified the oxide scale adhesion on Si-containing recycled hot-rolled steel by integrating metallurgical characterization with analytical fracture mechanics. Moving beyond qualitative observations, this study establishes a deeper understanding of the mechanical tenacity of scales in recycled alloys. The concluding insights are:

- Diffusion barrier and scale control: A consistent inverse relationship was established between the Si content and scale thickness. While the barrier effect of silicon (Si) is recognized in high-purity alloys, this study confirms that in recycled steel, despite the presence of residual impurities, the Si-oxide phase effectively acts as a diffusion barricade. This validates the role of Si in limiting material waste during high-temperature processing.
- Quantification of interfacial tenacity: A significant contribution of this work is the quantification of adhesion energy, which reached up to 40 J/m^2 in 0.3 wt.% Si steel. This value represents an important increase compared to the reported adhesion energy of Si-free low-carbon steels in existing literature. The formation of a stable, solid-state fayalite (Fe_2SiO_4) phase creates a mechanical anchoring effect that stabilizes the interface, providing a quantitative benchmark for the red scale phenomenon often described only qualitatively in previous works.
- Stress synergy and failure mechanics: This research clarifies the competition between interfacial bond strength and internal driving forces. It was found that at elevated temperatures (900 °C), the accumulation of internal thermal stress (driven by CTE mismatch and increased scale thickness) acts as a mechanical pre-load. This internal energy effectively overcomes the enhanced bonding provided by Si-anchors, explaining the observed reduction in critical strain. This insight links metallurgical phase stability with fracture mechanics to predict scale spallation behavior more accurately.
- Novel industrial threshold for recycled steel: This study identifies a critical Si threshold of 0.2 wt.% as a substantial transition point for managing scale adhesion in recycled steel grades. While earlier research focused on pure Fe-Si binaries, the findings of this study provide a practical industrial guideline that accounts for the complex compositions of recycled inputs. This threshold serves as a novel benchmark for producers to balance the trade-off between reducing material waste (thinner scale) and optimizing energy efficiency (descaling difficulty).

In summary, this work bridges the gap between theoretical adhesion models and industrial hot-rolling reality. The novelty lies in providing the first analytical quantification of adhesion energy for Si-containing recycled steel, offering a predictive framework that allows steel producers to optimize descaling processes, a crucial advancement for the sustainability of the circular steel economy.

ACKNOWLEDGMENT

This research was funded by the Faculty of Engineering, King Mongkut's University of Technology North Bangkok (Contract No. ENG-66-134).

REFERENCES

[1] C. Wang, H. Wu, and Y. Zhang, "Microstructure and Texture Evolution of the Oxide Scale on Hot Rolled Corrosion-resistant Steel," *Journal of Materials Research and Technology*, vol. 37, pp. 1541–1551, July 2025, https://doi.org/10.1016/j.jmrt.2025.06.129.

[2] K. Min, K. Kim, S. K. Kim, and D.-J. Lee, "Effects of Oxide Layers on Surface Defects During Hot Rolling Processes," *Metals and Materials International*, vol. 18, no. 2, pp. 341–348, Apr. 2012, https://doi.org/10.1007/s12540-012-2020-8.

[3] F. Gongye *et al.*, "Study on the Removal of Oxide Scale Formed on 300 M Steel Special-Shaped Hot Forging Surfaces during Heating at Elevated Temperature by a High-Pressure Water Descaling Process," *Materials*, vol. 16, no. 4, Feb. 2023, Art. no. 1745, https://doi.org/10.3390/ma16041745.

[4] T. P. Ojiako, M. F. Buchely, S. Lekakh, R. J. O'Malley, R. Osei, and T. Tayebali, "Parametric Analysis of Water Jet Descaling Efficiency of Reheated Continuously Cast Thin Slab," *Steel Research International*, Aug. 2025, Art. no. 2500481, https://doi.org/10.1002/srin.202500481.

[5] Q. Yuan, G. Xu, M. Zhou, and B. He, "The Effect of the Si Content on the Morphology and Amount of Fe_2SiO_4 in Low Carbon Steels," *Metals*, vol. 6, no. 4, Apr. 2016, Art. no. 94, https://doi.org/10.3390/met6040094.

[6] M. Zhou, G. Xu, H. Hu, Q. Yuan, and J. Tian, "The Morphologies of Different Types of Fe_2SiO_4–FeO in Si-Containing Steel," *Metals*, vol. 7, no. 1, Dec. 2016, Art. no. 8, https://doi.org/10.3390/met7010008.

[7] A. Paúl, S. El-Mrabet, and J. A. Odriozola, "High Temperature Oxidation of a High N, High Si, Mn Free Austenitic Stainless Steel," *Materials Science Forum*, vol. 383, pp. 125–130, Dec. 2001, https://doi.org/10.4028/www.scientific.net/MSF.383.125.

[8] A. Paúl, R. Sánchez, O. M. Montes, and J. A. Odriozola, "The Role of Silicon in the Reactive-Elements Effect on the Oxidation of Conventional Austenitic Stainless Steel," *Oxidation of Metals*, vol. 67, no. 1–2, pp. 87–105, Jan. 2007, https://doi.org/10.1007/s11085-006-9046-6.

[9] L. J. Yue and W. G. Chen, "The Corrosion Mechanism of Cu-Containing Weathering Steel in a Cyclic Dry-Wet Condition," *Advanced Materials Research*, vol. 79–82, pp. 957–960, Aug. 2009, https://doi.org/10.4028/www.scientific.net/AMR.79-82.957.

[10] P. E. Waudby, "Rare Earth Additions to Steel," *International Materials Reviews*, vol. 23, no. 1, pp. 74–98, Jan. 1978, https://doi.org/10.1179/imr.1978.23.1.74.

[11] H. Liu, L.-X. Du, J. Hu, H.-Y. Wu, X.-H. Gao, and R. D. K. Misra, "Interplay Between Reversed Austenite and Plastic Deformation in a Directly Quenched and Intercritically Annealed 0.04C-5Mn Low-Al Steel," *Journal of Alloys and Compounds*, vol. 695, pp. 2072–2082, Feb. 2017, https://doi.org/10.1016/j.jallcom.2016.11.046.

[12] J. Lee, W. Noh, D.-J. Kim, and M.-G. Lee, "Spallation Analysis of Oxide Scale on Low Carbon Steel," *Materials Science and Engineering: A*, vol. 676, pp. 385–394, Oct. 2016, https://doi.org/10.1016/j.msea.2016.09.012.

[13] S. Arrieta and S. Cicero, "Advances in Fracture, Fatigue and Structural Integrity Analyses of Metals," *Metals*, vol. 13, no. 5, May 2023, Art. no. 954, https://doi.org/10.3390/met13050954.

[14] H. E. Evans, "Stress Effects in High Temperature Oxidation of Metals," *International Materials Reviews*, vol. 40, no. 1, pp. 1–40, Jan. 1995, https://doi.org/10.1179/imr.1995.40.1.1.

[15] H. E. Evans, "Predicting Oxide Spallation from Sulphur-Contaminated Oxide/Metal Interfaces," *Oxidation of Metals*, vol. 79, no. 1–2, pp. 3–14, Feb. 2013, https://doi.org/10.1007/s11085-012-9322-6.